arXiv:1408.6802v2 [hep-ex] 26 Nov 2014

Noname manuscript No.
(will be inserted by the editor)

A method to measure the absolute branching fractions of Λ_c decays

A. Contu, D. Fonnesu, R.G.C. Oldeman, B. Saitta and C. Vacca

Received: 28 August 2014

Abstract It is proposed to exploit the decay of the meson $\mathrm{B}^+ \to p\pi^+\pi^+\overline{\Sigma}_c^{--}$ and of its charge conjugate B^- copiously produced at LHC to obtain a sample of Λ_c baryons through the strong decay $\Sigma_c \to \Lambda_c\pi$. The sample thus obtained is not affected by biases typically introduced by selections that depend on specific decay modes. Therefore it allows a measurement of the absolute branching fraction for the decay of the Λ_c baryon into $pK\pi$ or into other observable final states to be performed in a model independent manner. The accuracy that can be achieved with this method is discussed and it is shown that it would be either competitive with or an improvement over current measurements.

1 Introduction

Recently the Belle collaboration [1] has reported a value of $(6.84 \pm 0.24^{+0.21}_{-0.27})\%$ for the absolute branching fraction of the decay $\Lambda_c \to pK\pi$, obtained from the reconstruction of the system $D^*\bar{p}\pi$ recoiling against the Λ_c produced in e^+e^- annihilation. This measurement is model independent and has a significantly better precision than earlier results by the CLEO [2] and the ARGUS [3] collaborations, which were deduced making model dependent assumptions and are marginally consistent with one another.

In this paper it is suggested to exploit a particular decay of charged B mesons, produced with high yield at LHC, to measure the absolute branching fraction for the decay Λ_c into $Kp\pi$ - or any other observable decay mode - also in a model independent manner. The proposed method has the additional advantage of being applicable in a hadron collider environment since it does not require the reconstruction of the complete event. The paper is organised as follows. In Section 2 a description is given of the principle at the basis of the proposed method and in Section 3, by means of a simulation, the relations imposed by kinematics are exploited. In Section 4 selection efficiencies are evaluated, using the geometrical setup and quoted performance of the LHCb detector [4], to demonstrate the intrisic feasibility of the proposed measurement. The effects of non-resonant B-decays into the same final state are also discussed. In Section 5 the accuracy achievable with current data or with data available in the near future at LHC is evaluated.

2 Principle of Λ_c reconstruction

Even though the measured branching fraction of the decay $\mathrm{B}^+ \to p\pi^+\pi^+\overline{\Sigma}_c^{--}$ is only $2.8{\cdot}10^{-4}$ [5] the abundant production of charged B-mesons at LHC makes it possible to obtain samples containing $\mathrm{O}(10^7 - 10^8)$ decays of this type. The method proposed in this paper takes advantage of the decay chain $\mathrm{B}^+ \to p\pi^+\pi^+\left(\overline{\Sigma}_c^{--} \to \overline{\Lambda}_c^-\pi^-\right)$ whose diagram is shown in Fig. 1, to measure absolute Λ_c branching fractions [1] . The principle

Dipartimento di Fisica Università di Cagliari and INFN, Sezione di Cagliari, Italy

[1] Unless otherwise indicated, charge conjugation is implicitely assumed throughout.

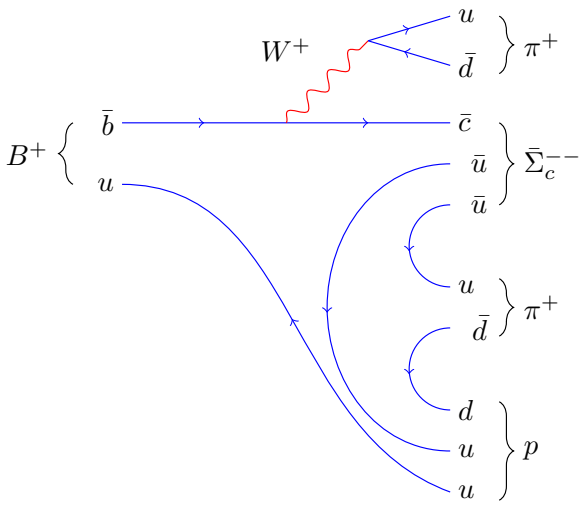

Fig. 1 Scheme of the decay $\mathrm{B}^+ \to p\pi^+\pi^+\overline{\Sigma}_c^{--}$.

which the method relies upon is based on the kinematics of the decay itself and is summarised in the following. Assume that in the decay all charged particles are observed with the exception of the Λ_c. If the direction of flight of the B-meson is known, it is possible to infer the existence of the Λ_c and to determine its momentum [2] without observing its decay, thus generating an unbiased sample of Λ_c's in which one would search for the mode whose branching fraction is sought to be measured.

The decay vertex of the B^+ (B^-) is identified by the presence of four charged particles (4-prong decay), namely $p\pi^+\pi^+\pi^-$ ($\bar{p}\pi^-\pi^-\pi^+$), having a total charge of $+2(-2)$. The B meson direction of flight is determined from the line joining the production (primary) and decay vertices.

Furthermore, the pion whose sign of charge is opposite to that of the three remaining particles certainly originates from the decay of Σ_c through strong interactions and, in what follows, it will be referred to as pion from Σ_c, π_Σ. In addition the presence of a proton would serve the purpose of tagging the decays of interest in experiments with good particle identification.

The B-meson decay vertex will be measured with an accuracy which depends on the experiment and is separated from the production vertex by a distance which would depend on the momentum spectrum of the B. The separation between the production and decay vertex and hence the direction of flight of the B-meson will be measured with an experiment dependent accuracy as well. These factors will be taken into account in Section 4.

Let $\hat{e}_B$ be a unit vector in the B direction of flight and $P_4 = (E_4, \mathbf{p}_4)$ (P_4^*) be the resultant four-momentum of all charged particles at the B-decay vertex - not including the Λ_c - in the laboratory frame (B rest frame). P_3 and P_3^* are the corresponding quantities of the three like-sign particles at the same vertex. Let the invariant mass of the two systems be M_4 and M_3 respectively and γ be the Lorentz γ-factor of the decaying B-meson.

Assuming that a Λ_c is the only missing particle in the decay, through simple algebra, it can be shown that the following two solutions are obtained for γ depending on whether the system of four-particles moves forward or backward in the B rest frame

$$\gamma_{1,2} = \frac{E_4 \cdot E_4^* \mp |\mathbf{p}_4^L| \cdot |\mathbf{p}_4^{*L}|}{M_4^2 + |\mathbf{p}_4^{*T}|^2} \tag{1}$$

where $\mathbf{p}_4^T$ and $\mathbf{p}_4^L$ are the transverse and longitudinal momentum with respect to the B-flight direction and E_4^*, the energy of the system of four particles in the B rest frame, is determined by the relation

[2] Up to a quadratic ambiguity.

$$E_4^* = \frac{M_B^2 - M_{\Lambda_c}^2 + M_4^2}{2M_B}$$

Hence $E_B = \gamma \cdot M_B$ and $\mathbf{P}_B = \sqrt{(E_B^2 - M_B^2)}\,\hat{e}_B$, since the B flight direction in known. The Λ_c four-momentum will be determined by imposing conservation of energy and momentum, $P_\Lambda = P_B - P_4$, and therefore, if the Λ_c truly originates from a Σ_c decay, its momentum would be such that the combination $(P_\Lambda + P_{\pi_\Sigma})^2$ must be equal to the Σ_c mass squared.

This should result in a peaking of the mass distribution around the true value of the Σ_c mass when the correct choice for the Lorentz γ factor has been made.

In this manner, an unbiased sample of Λ_c could be selected without actually observing the decay products of that particle and therefore it would be sufficient to identify within it the presence of decays into $pK\pi$ to measure the absolute branching fraction.

3 Feasibility of the proposed method

To demonstrate the viability of the proposed method, *pp* interactions were generated at centre of mass energy of 14 TeV, using the PYTHIA generator [6]. B^+, produced over the whole solid angle, were forced to decay in the channel of interest $\mathrm{B}^+ \to p\pi^+\pi^+\overline{\Sigma}_c^{--}$ using the software package EVTGEN [7]. Different samples in which the decay was of the non-resonant types $\mathrm{B}^+ \to p\pi^+\pi^+\pi^-\overline{\Lambda}_c^-$ and $\mathrm{B}^+ \to p\pi^+\pi^+\pi^-\overline{\Lambda}_c^-\pi^0$ were also generated to investigate possible kinematical variables which allow to separate the different decays.

There are indeed specific experimental advantages in using the suggested decay chain, some of which can be exploited by detectors with excellent particle identification, namely:

i) The four-prong decay vertex has charge +2. It is therefore relatively easy to identify and, in real experimental conditions, would help in reducing background from decays of particles other than the B^+.

ii) There is a proton at this vertex and therefore it can be efficiently identified to tag the B^+ decay. Furthermore, the charge of this proton is opposite to that of the proton from Λ_c decays and therefore no bias is introduced from a specific Λ_c decay mode.

iii) The pion from the Σ_c has sign of charge opposite to that of the other three particles and therefore it can be unambiguously distinguished.

iv) Conditions that events lie within kinematical boundaries can be applied in the selection to separate decays that occur through the resonance Σ_c from the non-resonant mode $\mathrm{B}^+ \to p\pi^+\pi^+\pi^-\overline{\Lambda}_c^-$, which has a branching fraction about 8 times larger, or from $\mathrm{B}^+ \to p\pi^+\pi^+\pi^-\overline{\Lambda}_c^-\pi^0$. In fact, if the final state $\bar{\Lambda}_c^-\pi^- p\pi^+\pi^+$ is reached via the resonance $\bar{\Sigma}_c^{--}$, M_4 should have values between the minimum

$$(M_4^2)_{min} = (E_3^{'} + E_{\pi_\Sigma}^{'})^2 - (\sqrt{E_3^{'2} - M_3^2} + \sqrt{E_{\pi_\Sigma}^{'2} - m_{\pi_\Sigma}^2})^2$$

and the maximum

$$(M_4^2)_{max} = (E_3^{'} + E_{\pi_\Sigma}^{'})^2 - (\sqrt{E_3^{'2} - M_3^2} - \sqrt{E_{\pi_\Sigma}^{'2} - m_{\pi_\Sigma}^2})^2$$

where $E_3^{'}$ and $E_{\pi_\Sigma}^{'}$ are the energies, in the Σ rest frame, of the system of three-particles and of the π_Σ, respectively.

Fig.2 shows the kinematic boundaries defined above in the *Dalitz-plane* $(M_4^2 - M_3^2)$. Decays in which a Σ_c is present fall within these boundaries and are shown by the shaded area, while within the contour lines are contained the indicated fractions of non-resonant decays $\mathrm{B}^+ \to p\pi^+\pi^+\pi^-\overline{\Lambda}_c^-$ (a) and $\mathrm{B}^+ \to p\pi^+\pi^+\pi^-\overline{\Lambda}_c^-\pi^0$ (b). The fraction of such decays within the kinematic boundaries is $(21.98 \pm 0.02)\%$ for $\mathrm{B}^+ \to p\pi^+\pi^+\pi^-\overline{\Lambda}_c^-$ and $(50.46 \pm 0.03)\%$ for the $\mathrm{B}^+ \to p\pi^+\pi^+\pi^-\overline{\Lambda}_c^-\pi^0$ mode. In Section 4 a quantitative estimate of the contribution from these decay modes will be given, once further selections have been applied. At this stage it is sufficient to observe that requiring a minimum value of M_3^2 and M_4^2 would be effective in reducing the fraction of non resonant decays, in particular of $\mathrm{B}^+ \to p\pi^+\pi^+\pi^-\overline{\Lambda}_c^-\pi^0$ whose branching fraction is not measured at present and only an upper limit exists [5].

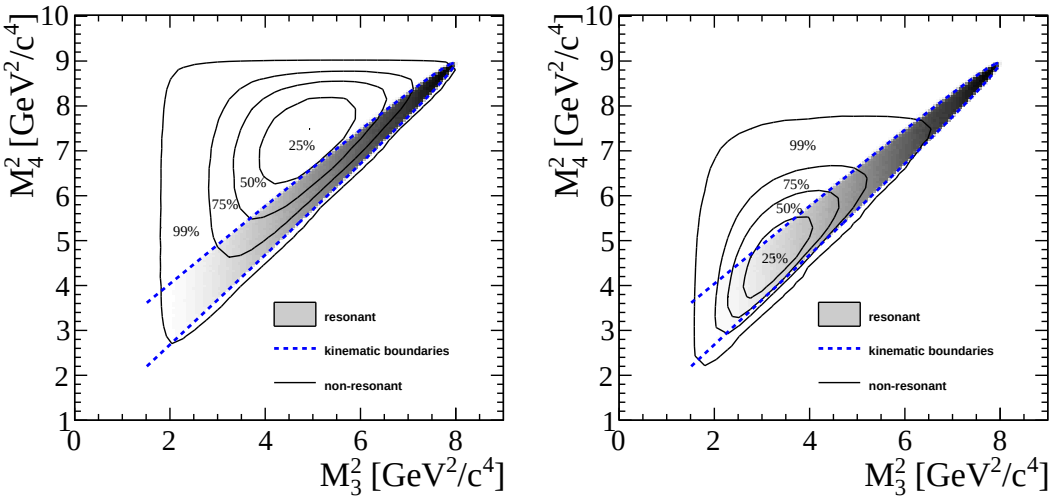

(a) Non resonant decay $B^+ \to p\pi^+\pi^+\pi^-\overline{\Lambda}_c^-$ (b) Non resonant decay $B^+ \to p\pi^+\pi^+\pi^-\overline{\Lambda}_c^-\pi^0$

Fig. 2 Distribution of the 4-particle invariant mass squared versus 3-particle invariant mass squared in resonant $B^+ \to p\pi^+\pi^+\overline{\Sigma}_c^{--}$ and non-resonant $B^+ \to p\pi^+\pi^+\pi^-\overline{\Lambda}_c^-$ and $B^+ \to p\pi^+\pi^+\pi^-\overline{\Lambda}_c^-\pi^0$ decays. The dashed line represents the kinematics boundaries for the resonant decay, while within the contour lines are contained the indicated fractions of non-resonant decays.

Detector acceptance was simulated in a simple manner, by assuming that particles with momentum greater than 2 GeV/c and within the pseudo-rapidity range $2 < \eta < 4.5$ would be detectable, as it would be approximately the case in the LHCb experiment, whose simplified setup will be used to estimate efficiencies. In the decay $B^+ \to p\pi^+\pi^+\left(\overline{\Sigma}_c^{--} \to \overline{\Lambda}_c^-\pi^-\right)$, the spatial distributions of particles are generated according to phase space, therefore, at generator level, there is no preferential direction for the Λ_c in the B rest frame. However, requiring that the decay products - other than the Λ_c - be within a detector acceptance, introduces asymmetries of order of 20%. This is shown in Fig. 3, where the distributions of the cosine of the angle between the direction of the momentum of the Λ_c in the B rest frame and the B direction of flight in various situations are compared.

There are indeed also losses introduced by this selection and these will be included in the efficiencies discussed in Section 4. At this stage it is sufficient to observe that requiring that the three like-sign particles be in acceptance favours slightly backward-going Λ_c's, while the further requirement that the pion from Σ_c be measurable, i.e. within the geometrical acceptance as well, would preferentially select forward-going Λ_c, as shown by the dashed lines in Fig. 3.

This selection of different regions of phase space will have an effect on the preferred value for the Lorentz γ factor. In fact, with the definition given in Eq. 1, γ_1 is always smaller than γ_2 and therefore chosing the first over the latter selects B's of lower energy. If for instance experimental acceptance is such that forward going Λ_c are slightly favoured, then γ_2 would be more often the correct solution. On the other hand, additional selections - that might prove necessary when dealing with the real experimental conditions - are likely to change the favoured value. However this would have no effect on the proposed measurement, as long as no bias is introduced by the decay mode of the Λ_c, which is the case here since the Λ_c decay products are not and will not be considered in the selection.

For each event, the two values of the Lorentz γ factor given by Eq. 1 are computed using true quantities at generator level. $\sqrt{(P_\Lambda + P_{\pi_\Sigma})^2}$ is then computed assuming, as solution, either γ_1 or γ_2. The mass distribution obtained in this manner is shown in Fig. 4 as solid histogram. As already mentioned there is complete symmetry forward-backward at this stage and therefore chosing either solution, γ_1 or γ_2, leads to the same result. As expected, a peak around the Σ_c mass is observed. Its width is affected by the cases in which the

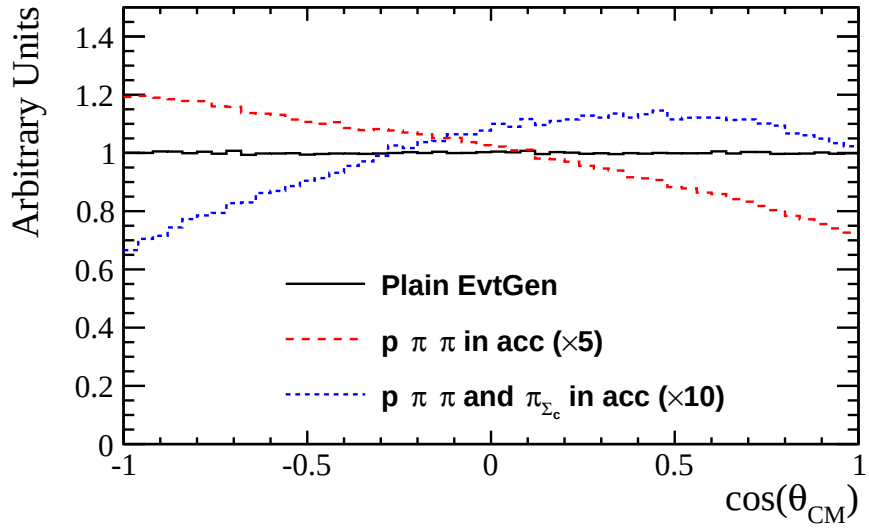

Fig. 3 Angular distributions of the Λ_c baryon in the B rest frame before and after applying selection criteria

wrong solution for γ was chosen, yet the result was close to its true value and, as a consequence, a value about 10% larger than expected is observed [3] .

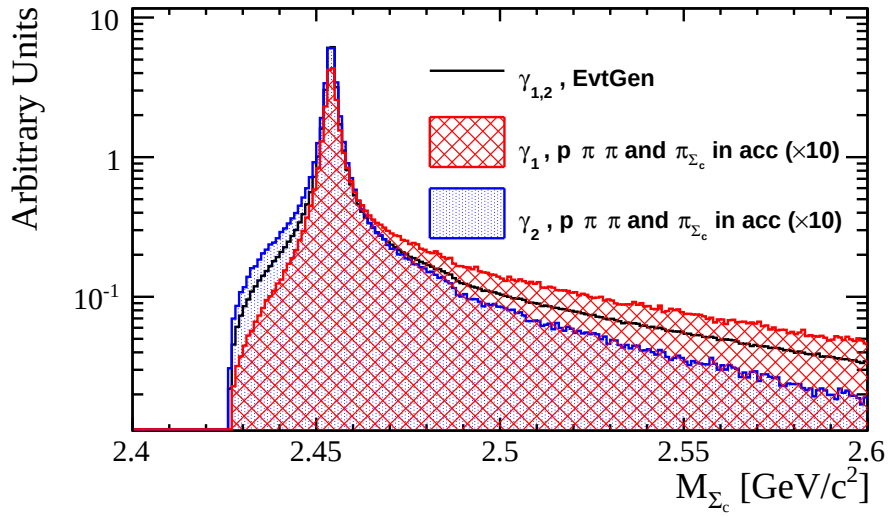

Fig. 4 Distributions of the reconstructed $\bar{\Sigma}_c^{--}$ mass before and after applying selection criteria.

Using either value of γ and requiring 2.44 $GeV/c^2 < M_\Sigma <$ 2.47 GeV/c^2, would allow a selection of a sample of Λ_c whose size is about 64% of the original sample of generated events. On the other hand chosing particles that fall within the geometrical acceptance would produce different mass distributions for the two choices of γ, as illustrated in Fig. 4 with slightly different efficiencies which will be discussed quantitatively in Section 4.

Even though the choice of γ_1 or of γ_2 is irrelevant since either one would allow the selection of an unbiased sample of Λ_c's, efficiencies are different and this would affect the size of the final sample and ultimately the statistical accuracy. To minimize the statistical error on the measurement, it would be required in addition

[3] At this level, if the correct solution were chosen, one would expect to obtain a width of 2.6 MeV/c^2 for the Σ_c, which is the value coded in the Montecarlo.

that the decay products of the Λ_c be detected and hence it is the number of observable decays that ought to be maximized.

4 Effects of experimental resolution and efficiencies

Experimental resolution on the determination of momenta of particles and of positions of vertices so far have not been taken into account. To estimate its effect, a simplified geometrical setup of the LHCb experiment was used in the Montecarlo simulation. Therefore the momentum-dependent smearing quoted in ref. [9] (which corresponds to $\delta P/P \sim 0.4\%$ for a particle with $P = 10\ GeV/c$) was applied to particle momenta and gaussian smearings of $\sigma_z = 400\mu m$ along the beam direction and of $\sigma_T = 35\mu m$ in the transverse beam direction were applied to the position of the B decay vertex [8]. It was found that, of the two, the error on the vertex position has the largest effect since it enters in the determination of the B direction of flight. The effect is shown in Fig. 5 where the M_{Σ_c} distribution is displayed for the γ_2 solution and all four-particles within the geometrical acceptance, assuming the true B-direction or that obtained having applied only the smearing on the B-decay vertex. The result is essentially unchanged when the momentum smearing is also applied. The effect of the experimental resolution is to reduce the event sample to about 45% of its original size and it is mostly due to the fact that the transverse momentum relative to the *measured* B-direction exceeds the maximum value allowed by kinematics and hence no acceptable solutions for γ are found.

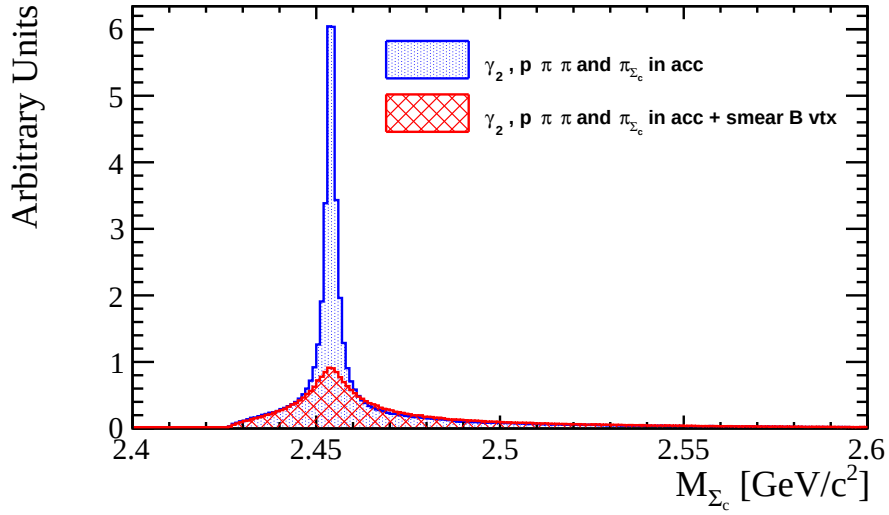

Fig. 5 Distributions of the reconstructed $\bar{\Sigma}_c^{--}$ mass before and after applying resolution smearing.

Tables 1 and 2 summarise the effects of the selections listed below and applied to the $B^+ \to p\pi^+\pi^+\overline{\Sigma_c}^{--}$ sample as well as to the *non-resonant* samples, i.e. to the samples of events in which the final state $\Lambda_c\pi p\pi\pi$, with or without the presence of an additional neutral pion, is reached directly from B decay and not via the resonance Σ_c for the two possible choices of γ:

- Selection **A**: $(M_4^2)_{min} < M_4^2 < (M_4^2)_{max}$
- Selection **B**: Mass of the Σ_c, computed as $\sqrt{(P_\Lambda + P_{\pi_\Sigma})^2}$, is within $\pm 15\ MeV/c^2$ from its nominal value of 2.455 GeV/c^2.
- Selection **C**: $p\pi\pi$ like-sign within geometrical acceptance.
- Selection **D**: π_Σ within geometrical acceptance.
- Selection **E**: Smearing is applied to B-decay vertex.
- Selection **F**: $M_3^2 > 4(GeV/c^2)^2$ and $M_4^2 > 6(GeV/c^2)^2$

The criteria were applied in order, i.e. each selection implies that all the preceeding conditions were satisfied.

Table 1 Accepted solution γ_1 - Fraction of events kept

Condition	$B^+ \to p\pi^+\pi^+\overline{\Sigma}_c^{--}$	$B^+ \to p\pi^+\pi^+\pi^-\overline{\Lambda}_c^-$	$B^+ \to p\pi^+\pi^+\pi^-\overline{\Lambda}_c^-\pi^0$
Selection **A**	1	$(21.98 \pm 0.02) \cdot 10^{-2}$	$(50.46 \pm 0.03) \cdot 10^{-2}$
Selection **B**	$(62.19 \pm 0.03) \cdot 10^{-2}$	$(1.986 \pm 0.005) \cdot 10^{-2}$	$(2.493 \pm 0.006) \cdot 10^{-2}$
Selection **C**	$(6.501 \pm 0.009) \cdot 10^{-2}$	$(2.00 \pm 0.02) \cdot 10^{-3}$	$(2.39 \pm 0.02) \cdot 10^{-3}$
Selection **D**	$(2.554 \pm 0.006) \cdot 10^{-2}$	$(6.89 \pm 0.09) \cdot 10^{-4}$	$(3.03 \pm 0.06) \cdot 10^{-4}$
Selection **E**	$(1.055 \pm 0.004) \cdot 10^{-2}$	$(3.79 \pm 0.07) \cdot 10^{-4}$	$(2.76 \pm 0.06) \cdot 10^{-4}$
Selection **F**	$(8.52 \pm 0.03) \cdot 10^{-3}$	$(2.96 \pm 0.06) \cdot 10^{-4}$	$(1.07 \pm 0.04) \cdot 10^{-4}$

Table 2 Accepted solution γ_2 - Fraction of events kept

Condition	$B^+ \to p\pi^+\pi^+\overline{\Sigma}_c^{--}$	$B^+ \to p\pi^+\pi^+\pi^-\overline{\Lambda}_c^-$	$B^+ \to p\pi^+\pi^+\pi^-\overline{\Lambda}_c^-\pi^0$
Selection **A**	1	$(21.98 \pm 0.02) \cdot 10^{-2}$	$(50.46 \pm 0.03) \cdot 10^{-2}$
Selection **B**	$(64.02 \pm 0.04) \cdot 10^{-2}$	$(2.014 \pm 0.005) \cdot 10^{-2}$	$(2.581 \pm 0.006) \cdot 10^{-2}$
Selection **C**	$(5.784 \pm 0.009) \cdot 10^{-2}$	$(1.94 \pm 0.02) \cdot 10^{-3}$	$(2.17 \pm 0.02) \cdot 10^{-3}$
Selection **D**	$(3.403 \pm 0.007) \cdot 10^{-2}$	$(1.29 \pm 0.01) \cdot 10^{-3}$	$(1.79 \pm 0.02) \cdot 10^{-3}$
Selection **E**	$(1.536 \pm 0.004) \cdot 10^{-2}$	$(8.3 \pm 0.1) \cdot 10^{-4}$	$(1.43 \pm 0.01) \cdot 10^{-3}$
Selection **F**	$(1.117 \pm 0.004) \cdot 10^{-2}$	$(5.62 \pm 0.08) \cdot 10^{-4}$	$(3.49 \pm 0.07) \cdot 10^{-4}$

From the tables it can be concluded that efficiencies at the percent level for the indicated selections are obtained and that, as expected, γ_2 would be the favoured solution when requiring that π_Σ be within geometrical acceptance (i.e. having pseudo-rapidity in the range $2 < \eta < 4.5$, as previously defined).

As it was also expected, the requirements imposed on kinematics and detector geometry are less effective for the non-resonant channels, the efficiencies being smaller by a factor of about 20. This reduction will be partly compensated for by the larger B-decay branching fraction into these channels. Quantitatively this is shown in Fig. 6 where the Σ_c mass distribution is displayed for the resonant and non-resonant channels properly weighted with the B-decay branching fractions and the efficiencies quoted in Table 2 for the selection **A**. For the decay $B^+ \to p\pi^+\pi^+\pi^-\overline{\Lambda}_c^-\pi^0$, since only an upper limit exists for the branching fraction, it was assumed to be equal to that of $B^+ \to p\pi^+\pi^+\pi^-\overline{\Lambda}_c^-$. In the mass range $2.44 - 2.47$ GeV/c^2,considered as the signal region, the total non-resonant fraction, with the above assumption, is $\sim 36\%$ of the total. In real experimental conditions this signal would be superimposed to a combinatorial background, therefore it would not be meaningful at this stage to extract a function describing its shape.

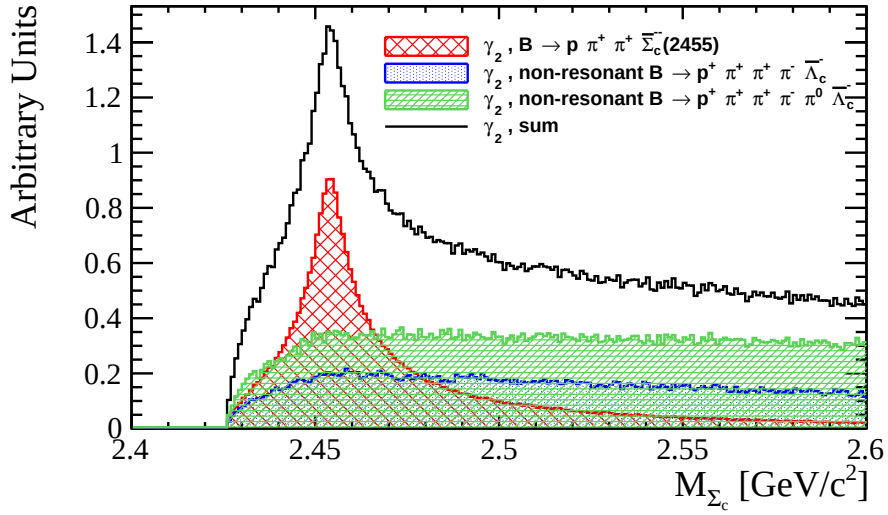

Fig. 6 Distributions of the reconstructed $\bar{\Sigma}_c^{--}$ mass in resonant ($B^+ \to p\pi^+\pi^+\overline{\Sigma}_c^{--}$) and non-resonant decays ($B^+ \to p\pi^+\pi^+\pi^-\overline{\Lambda}_c^-$ and $B^+ \to p\pi^+\pi^+\pi^-\overline{\Lambda}_c^-\pi^0$).

As already pointed out, it is the number of observable decays that should be maximised. Table 3 shows, for the decay $\Lambda_c \to pK\pi$, the fraction of events, satisfying the indicated selections, in which the decay products of the Λ_c are also within geometrical acceptance, both for the resonant and non-resonant components. Efficiencies are of order of $\sim 40\%$ irrespective of the choice of γ and depend weakly on whether the Λ_c is produced directly from B decay or through the Σ_c resonance. This was to be expected, since essentially only geometrical factors enter in the determination of these fractions.

Table 3 Fraction of events for the indicated selections in which the Λ_c decay products are also within geometrical acceptance

Condition	$B^+ \to p\pi^+\pi^+\overline{\Sigma}_c^{--}$	$B^+ \to p\pi^+\pi^+\pi^-\overline{\Lambda}_c^-$	$B^+ \to p\pi^+\pi^+\pi^-\overline{\Lambda}_c^-\pi^0$
Selection **D** and Solution γ_1	39.82 ± 0.12	42.6 ± 0.8	40.9 ± 1.1
Selection **E** and Solution γ_1	39.17 ± 0.18	40.7 ± 1.0	41.5 ± 1.1
Selection **F** and Solution γ_1	39.16 ± 0.2	41.4 ± 1.1	42.3 ± 1.9
Selection **D** and Solution γ_2	40.54 ± 0.10	41.4 ± 0.5	39.5 ± 0.4
Selection **E** and Solution γ_2	40.03 ± 0.15	40.3 ± 0.6	39.8 ± 0.5
Selection **F** and Solution γ_2	40.04 ± 0.18	41.9 ± 0.8	41.8 ± 1.0

5 Results and Conclusions

LHCb has measured a cross section of 38.9 μb for the production of charged B mesons within the experimental acceptance and with transverse momentum in the range $0 - 40$ GeV/c [10], in pp collisions at centre of mass energy of 7 TeV. This would correspond to a cross section of $193\mu b$ over the whole solid angle, assuming that B-mesons are produced as in PYTHIA generator. Scaling the production cross-section with $\sqrt{s}$, this would yield about $3.9 \cdot 10^{11}$ charged B-decays per fb^{-1} of integrated luminosity.

Selecting, for the sake of illustration, the efficiencies corresponding to the γ_2 solution in Table 2 and assuming that these do not have a strong dependence on the pp centre-of-mass energy, using an integrated luminosity of 3 fb^{-1} (currently available in the LHCb experiment at centre of mass energies of 7 and 8 TeV), with the measured branching fraction of $2.8 \cdot 10^{-4}$ for $B^+ \to p\pi^+\pi^+\overline{\Sigma}_c^{--}$, about 2.5 million decays of interest would be *reconstructed* within the detector: a sizeable, unbiased sample of Λ_c decays.

However, to obtain a more realistic estimate of the above number, the effects of other selections which is necessary to apply and have not been considered here, should be included. These in general are functions of transverse momentum and pseudo-rapidity and efficiencies have typically the values quoted in Ref. [11]. Assigning the realistic value of 2% to account for all the effects not included in the simplified simulation, using the efficiencies of Table 3 for the Λ_c decay products, about 1000 decays of the type $\Lambda_c \to pK\pi$ from the resonant sample would be observed in the detector. The statistical error therefore would be comparable with that of Belle [1], which is the most precise currently available measurement.

The presence of large backgrounds could spoil the effectiveness of the proposed method. These can be estimated only through a detailed and complete simulation using a specific detector and it is beyond the scope of this article. However it should be observed that the choice was made - over other topologies which would have enlarged the sample - of a B-decay vertex of charge ± 2, with a well defined topology, separated from the primary pp interaction vertex, and containing a well identified proton, with the intent of reducing combinatorial background. Backgrounds from specific decays of B-mesons have been considered. In particular, as seen in Tables 1 and 2 and in Fig. 6, non-resonant decays $B^+ \to p\pi^+\pi^+\pi^-\overline{\Lambda}_c^-$ and $B^+ \to p\pi^+\pi^+\pi^-\overline{\Lambda}_c^-\pi^0$, contribute less than 40% to the total number. The decay $B^+ \to p\pi^+\pi^+\pi^-\overline{\Lambda}_c^-\pi^0$ with a missing neutral pion may be considered representative of the class of decays with topology identical to that of interest when one or more particles are missing. The validity of this statement was verified by considering in the simulation

also the decay $B^\circ \to p\pi^+\pi^+\pi^-\pi^-\overline{\Lambda}_c^-$, which would mimic the signal when missing a π^-. A fraction of about 3.7 10^{-4} of events of this type were found for selection **F**, in the mass region of interest. As expected, the retained fraction is similar to that accepted for the decay $B^+ \to p\pi^+\pi^+\pi^-\overline{\Lambda}_c^-$. The cross section for B° production is similar to that for charged B's [10]. However for the branching fraction of the decay considered here only an upper limit exists and therefore it would contribute to background at most $\sim 30\%$ of the resonant signal.

Systematic effects are experiment dependent as well and therefore can not be properly estimated in this paper. However it is worth noticing that the method relies on *counting* the observed number of $\Lambda_c \to pK\pi$ decays in a sample whose selection does not rely upon observation of the Λ_c decay products. Therefore most of the systematics would cancel when taking the ratio. The line shape used in the fit to determine the size of the initial, unbiased sample would be taken from Montecarlo simulation. The effects of the uncertainty on this shape would not cancel however and would most likely be the main source of systematic error. Particle identification (proton in particular) would be used to identify the Λ_c decay mode of interest. This would affect only the detection efficiency listed in Table 3 and therefore it would not cancel in the ratio and would become important if statistics were limited.

The overall result could be improved by devising dedicated, more efficient selections at trigger level and when more data and at higher centre of mass energy become available. Furthermore the decays from Λ_c's originating from the non-resonant channels could be added to the sample, since their detection efficiency is similar to that for Λ_c coming from the resonant channel and therefore large corrections would not be required.

References

1. A. Zupanc *et al.* [Belle Collaboration], Phys. Rev. Lett. 113 (2014) 042002.
2. T. Bergfeld *et al.* [CLEO Collaboration], Phys. Lett. B **323** (1994) 219 [hep-ph/9403326].
3. H. Albrecht *et al.* [ARGUS Collaboration], Phys. Lett. B **269** (1991) 234.
4. A. A. Alves Jr. *et al.*, [LHCb Collaboration], JINST **3** (2008) S08005.
5. J. Beringer *et al.* [Particle Data Group Collaboration], Phys. Rev. D **86** (2012) 010001 *and 2013 partial update for the 2014 edition* http://pdg.lbl.gov/
6. T. Sjostrand, S. Mrenna and P. Z. Skands, Comput. Phys. Commun. **178** (2008) 852 [arXiv:0710.3820 [hep-ph]].
7. D. J. Lange, Nucl. Instrum. Meth. **A462** (2001) 152.
8. R. Aaij *et al.*, JINST **9** (2014) P09007.
9. R. Antunes Nobrega. *et al.*, [LHCb Collaboration], LHCb - Technical Design Report, http://lhcb.web.cern.ch/lhcb/TDR/TDR9.pdf
10. R. Aaij *et al.* [LHCb Collaboration], JHEP **1308** (2013) 117.
11. R. Aaij *et al.* [LHCb Collaboration], Phys. Rev. D **85** (2012) 032008.